COMPARISON OF LOW COST PHOTOGRAMMETRIC SURVEY WITH TLS AND LEICA PEGASUS BACKPACK 3D MODELSS

A. Masiero[a, *], F. Fissore[a] , A. Guarnieri[a], M. Piragnolo[a], A. Vettore[a]

[a] Interdepartmental Research Center of Geomatics (CIRGEO), University of Padova,
Viale dell'Università 16, Legnaro (PD) 35020, Italy -
masiero@dei.unipd.it
(francesca.fissore, alberto.guarnieri, marco.piragnolo, antonio.vettore)@unipd.it

KEY WORDS: Low Cost 3D Reconstruction, Mobile Mapping, UWB, Backpack, Photogrammetry, Terrestrial Laser Scanning

ABSTRACT:

This paper considers Leica backpack and photogrammetric surveys of a mediaeval bastion in Padua, Italy. Furhtermore, terrestrial laser scanning (TLS) survey is considered in order to provide a state of the art reconstruction of the bastion. Despite control points are typically used to avoid deformations in photogrammetric surveys and ensure correct scaling of the reconstruction, in this paper a different approach is considered: this work is part of a project aiming at the development of a system exploiting ultra-wide band (UWB) devices to provide correct scaling of the reconstruction. In particular, low cost Pozyx UWB devices are used to estimate camera positions during image acquisitions. Then, in order to obtain a metric reconstruction, scale factor in the photogrammetric survey is estimated by comparing camera positions obtained from UWB measurements with those obtained from photogrammetric reconstruction. Compared with the TLS survey, the considered photogrammetric model of the bastion results in a RMSE of 21.9cm, average error 13.4cm, and standard deviation 13.5cm. Excluding the final part of the bastion left wing, where the presence of several poles make reconstruction more difficult, (RMSE) fitting error is 17.3cm, average error 11.5cm, and standard deviation 9.5cm. Instead, comparison of Leica backpack and TLS surveys leads to an average error of 4.7cm and standard deviation 0.6cm (4.2cm and 0.3cm, respectively, by excluding the final part of the left wing).

1. INTRODUCTION

Mobile mapping systems, based either on terrestrial/aerial vehicles or on human carried devices (El-Sheimy and Schwarz, 1998, Toth, 2001, Remondino et al., 2011, Masiero et al., 2016, Al Hamad and El Sheimy, 2014, Piras et al., 2017, Chiang et al., 2012, Masiero et al., 2015, Ballarin et al., 2017, Fissore et al., 2017, Guarnieri et al., 2015), have been used in the last dozen of years in order to map and monitor areas of interest in a quite range spread of applications.

Current generation of mobile mapping systems is mostly based on the use of GNSS positioning method and either laser scanning or photogrammetric reconstruction. Despite the very accurate positioning accuracy that can be obtained outdoors by using high grade GNSS receivers, their results in indoor environments (and also in certain outdoor environments, e.g. close to high buildings or mountains) are usually not sufficient for most of the applications of interest.

Given the high request for accurate metric reconstructions, positioning in such working conditions is typically obtained by integrating information provided by different sensors (e,g, inertial measurements provided by the Inertial Measurement Unit (IMU), acceleration, gyroscope and magnetometer measurements, vision, and WiFi, if available (Saeedi et al., 2014, Widyawan et al., 2012)). A recent example of mobile mapping system allowing accurate surveying also in indoor environments is the Leica Pegasus backpack. When GNSS positioning is not available/reliable, Leica Pegasus backpack allows positioning by integrating IMU and laser scanning measurements (acquired at different time instants).

This paper considers another method for positioning in environments challenging for GNSS: positioning based on the use of Ultra-Wideband (UWB) devices. More specifically, device position is obtained by means of range measurements, which can be directly derived by the times of flight of Ultra-Wideband (UWB) radio signals (as usual when dealing with range based positioning, four measurements from known positions (provided by devices not lying on a plane) are needed in order to enable 3D positioning, whereas three are enough for positioning on a planar surface (2D positioning)).

Similarly to IMU positioning, UWB allow to obtain position estimated with respect to a local coordinate system, however it has the advantage of not requiring external measurements to reduce any drift.

Pozyx UWB devices are used in this work: Interestingly, Pozyx devices are cheap with respect to other UWB systems on the market ($150 each, approximately). First, certain characteristics of systematic (and random) errors are shown: random noise is shown to be quite small (3 centimeters, approximately) hence potentially allowing positioning with an accuracy level of few centimeters. Systematic error has been previously modelled as a constant time lag (e.g. due to device synchronization) (Hol, 2011) and as a polynomial term, as a function of distance (Toth et al., 2015, Dierenbach et al., 2015, Goel et al., 2017). Actually, according to our experiments, systematic errors of the considered low cost Pozyx devices are significantly anisotropic, i.e. when aiming at fully exploiting the positioning potentiality of the UWB signals, dependence on the orientation of the device and on its direction (angle) with respect to the other UWB antennas is typically not negligible.

Taking into account of the above observations, a complete calibration of the UWB systematic error might be quite complicated for a non-specialized end user of the system. Motivated by this consideration, this paper aims at (partially) compensate the UWB systematic error while not requiring complicated calibration pro-

*Corresponding author.

cedures to the user, i.e. the rationale is that the system should be as simple as possible for the user.

The UWB positioning system, integrated with a photogrammetric reconstruction system (done both with calibrated and uncalibrated camera, i.e. self-calibration (Habib and Morgan, 2003, Heikkila and Silven, 1997, Remondino and Fraser, 2006, Fraser and Stamatopoulos, 2014, Luhmann et al., 2015)), can be considered as a stand-alone low cost surveying system (however georeferencing is not allowed without the integration of a GNSS receiver as well). The above described system is tested on an indoor surveying case study in Padova (Italy): the Impossibile bastion (Fig. 1), along the walls of Padova, where GNSS is clearly not available.

For comparison, surveys of other two methods are considered as well: the first obtained by using a Leica Pegasus backpack (Fig. 3(a)), whereas the second one with terrestrial laser scanning technique (obtained by using Leica ScanStation C10 (Remondino et al., 2005, Pirotti et al., 2013), Fig. 3(b)).

(a) (b)

Figure 1. (a) Top view of Impossibile bastion, walls of Padova, Italy. Terrestrial laser scanner 3D reconstruction obtained with Leica ScanStation C10. (b) Inside view of the bastion.

(a) (b)

Figure 2. (a) UWB Pozyx device powered by a standard powerbank. (b) Canon G7X camera.

Pegasus backpack is a terrestrial mobile mapping system recently developed by Leica: it features 2 laser profilers, 5 cameras, GNSS receiver and 200Hz Inertial Navigation System (INS). The rationale of that system is that of allowing accurate and relatively fast surveys of areas reachable by a human carrying a backpack and where carrying there other instrumentation might be impossible or difficult. The comparison between the results obtained by Pegasus backpack and our develop system is motivated by their common factors of interest: mobility, portability and possible usage in areas where GNSS is not available. Clearly, given the integration of more sensors (and the drastically different cost), performance of Pegasus backpack can be seen as an upper bound to these that might be obtained by the system proposed here.

Accuracy of the terrestrial laser scanning survey is expected to be better than that of both the other two methods, and its survey will be consequently considered as *ground truth*.

(a) (b)

Figure 3. (a) Leica Pegasus backpack. (b) Setup of the Leica ScanStation C10 over a traverse mark and target pole over the back target.

2. OBJECTIVES

The objective of this paper is the analysis of the performance of a mobile mapping solution based on the use of photogrammetry and low cost UWB devices. The considered UWB devices are Pozyx low cost indoor navigation solution. This goal is achieved through using map information to re-correct MEMS-based inertial sensors results using a two-layer structure PF/KF algorithm. Also, to balance between the estimation accuracy and the computational speed, three PFs, including SIS PF, APF, and BPF are designed and implemented in this paper.

3. UWB POSITIONING SYSTEM AND PHOTOGRAMMETRIC RECONSTRUCTION

Pozyx is a low cost UWB positioning system recently developed by Pozyx Lab [3] (first devices have been shipped in 2016). Two types of Pozyx devices can be distinguished, anchors and rovers. Anchors are assumed to be in a fixed and known position during all the navigation, whereas rovers can move in the environment. Goal of the system is that of providing estimates of rover positions based on range measurements of the distances between rovers and anchors. Interestingly, Pozyx devices are provided of an auto-detecting procedure that allows them to detect and communicate with each other. Once turned on, rovers and anchors start to communicate and to provide range measurements. Code executed by the rover can be easily personalized. In particular, in this case study just one rover was used to collect range measurements (positioning has been performed post-processing data). Nevertheless, it is worth to notice that software provided with the Pozyx system (and typically executed on an Arduino) allows also real time positioning. However, this functionality has not been used in our experiments in order to save computational power, and hence allowing a higher frequency for range collection. This choice is also motivated by the relatively limited computational power of Arduino Uno, which was used in this work in order to properly control the Pozyx rover. However, real time positioning shall be obtained also connecting the system described above with a device with more computational resources.

Pozyx devices are quite small (maximum side size is 6cm) and lightweight (12g, approximately), hence particularly well suited for mobile mapping applications. Thanks to their low power consumption they can be conveniently powered with standard powerbank batteries via a specific USB cable (see Fig. 2(a)).

Nominal characteristics of interest (and the values that has been obtained in our experiments) of Pozyx system are reported in the following table:

	Nominal values	Experimental values
range accuracy	10 cm	15cm
maximum range	100 m	55/120m
maximum update rate	80Hz	≈ 50Hz

It is worth to notice that actual values for the parameters reported above depend on several factors (e.g. environment and system settings). In particular, maximum range can drastically vary depending on the environment (and if operating conditions are indoors or outdoors, i.e. ≈ 50 m or 120 m, respectively, in our experiments).

Experimental range accuracy estimated in our tests (see also Fig. 2 in (Masiero et al., 2017)) is similar to the nominal one, and error distribution can be considered as zero-mean and approximately Gaussian.

An important factor is the rate of measurement acquisition (i.e. the number of measured ranges with respect to the number of times that such measurements have been required by the rover), that varies significantly depending on the range value, as shown in Fig. 4. Fig. 4 has been computed from data acquired during the survey at the Impossible bastion.

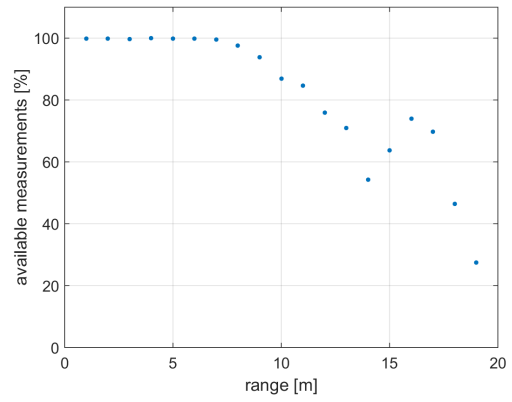

(a)

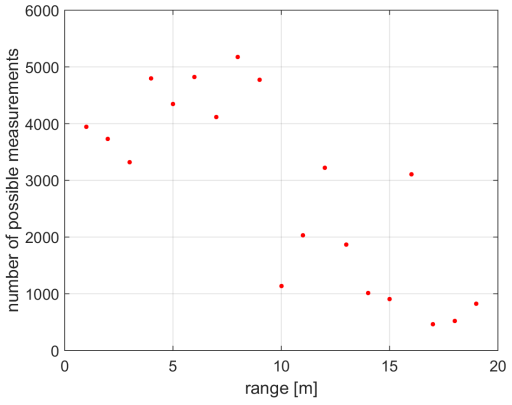

(b)

Figure 4. (a) Acquisition rate as a function of the range value. (b) Number of possible measurements considered to compute acquisition rates in (a).

Despite maximum range of Pozyx devices is substantially in accordance with the nominal value (actually it is even a bit higher), in fact their use shall be limited to much lower ranges when a high rate of range acquisitions has to be ensured.

Range update rate (per each anchor) is (linearly) inversely proportional to the number of considered anchors.

Anchor positions are assumed to be known to be able to solve the positioning problem. Range measurements can be combined by using an Extended Kalman Filter (EKF) in order to obtain estimates of the rover position.

In particular, in the case study considered in this work, four anchors were distributed as shown in Fig. 3 on the ground inside of the Impossibile bastion. Anchor positions have been measured by means of a Leica TCR 702 Total Station. However, it is worth to notice that the use of a total station might be difficult in certain environments/operating conditions. The validation of results that can be obtained by using alternative options in order to obtain estimates of anchor positions (e.g. self-positioning of anchors by means of their own measurements, native functionality included in the Pozyx system) is foreseen in our future investigations.

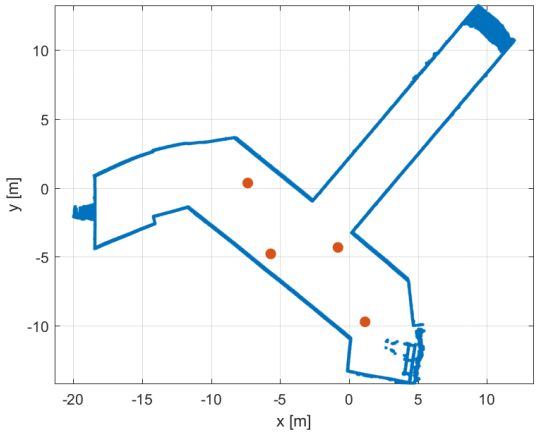

Figure 5. Pozyx anchor positions during survey in Impossibile bastion.

Rover has been attached to the camera used for photogrammetric reconstruction and they have been moved at approximately constant altitude during the survey. In particular, altitude with respect to the approximately planar surface where anchors were positioned was fixed at a constant value (h≈1.5 m) during image acquisitions in order to obtain best positioning results from the four anchors used during data collection in the bastion. Consequently, EKF has been formulated in order to track rover position on a planar surface at constant altitude. Dynamic is modeled as follows:

$$\begin{bmatrix} x_{t+1} \\ \dot{x}_{t+1} \end{bmatrix} = \begin{bmatrix} 1 & T \\ 0 & 1 \end{bmatrix} \begin{bmatrix} x_t \\ \dot{x}_t \end{bmatrix} + w_t \qquad (1)$$

where x_t is the rover 2D position at time t on the planar surface at constant altitude, T is the length of the time interval between the two estimates, and w_t is the model noise.

Measurement equation for anchor i is:

$$y_{t,i} = \sqrt{(x_{t,u} - q_{i,u})^2 + (x_{t,v} - q_{i,v})^2 + h^2} + z_t \qquad (2)$$

where $y_(t, i)$ is the measurement of anchor i at time t, q_i is the position of anchor i (u and v are two orthogonal direction onn the

horizontal plane), and z_t is the measurement noise. Future investigation foresees also the integration with pedestrian positioning estimation methods.

Images of the bastion have been taken by using a Canon G7X camera (20.2 MPix), with settings fixed at constant values (1/60s shutter speed, f/1.8 aperture, 8.8mm focal length, i.e. 35mm equivalent: 24mm). 335 images have been collected varying camera position and orientation in the bastion. Agisoft PhotoScan has been used in order to obtain a self-calibrated reconstruction of the bastion.

Then, the rationale is that of integrating photo-based 3D reconstruction with Pozyx estimates of camera positions in order to obtain a metric reconstruction. Estimate of 3D model scale has been obtained by computing the best (in least squares sense) rigid transformation (rotation, translation and scale) between the camera positions provided by PhotoScan and the corresponding ones estimated with the Pozyx system. In this process the same weight have been given to all positions estimated by the UWB system. However, positions far from UWB are clearly affected by a higher estimation error with respect to those surrounded by anchors. Introducing different weights depending on the considered position might improve scale estimation performance.

During each image acquisition camera has been firmly held for 2-3 seconds. Manual synchronization between camera and UWB measurements has been initially set taking into account of measurements provided by the inertial measurement unit (approximately still when taking images). Then, synchronization has been refined including it in the least squares minimization process previously considered for the scale estimation.

Photogrammetric and UWB data acquisition in the bastion lasted approximately a hour (on January 19^{th}, 2017), where most of such time was spent for acquiring a sufficient amount of images.

4. LEICA PEGASUS BACKPACK SURVEY

Leica Pegasus backpack survey was done on December 21^{st}, 2016 and lasted less than a hour: half a hour was spent for system setting up and calibration, whereas data acquisition required only few minutes. Hence, once calibrated Leica Pegasus allowed to complete the survey much faster than the system proposed in the previous Section. Clearly, this aspect can be a very important factor (and shall be more apparent) when surveying a larger area.

Weight of the Pegasus backpack ($\approx$ 13 kg) is surely higher than that of system considered in the previous Section, but it is acceptable (especially if it is used for a quite limited period of time).

The 2 laser profilers acquires 600k points per second (maximum range of 50 m), whereas Inertial Navigation System (INS) nominally ensures RMS of 20 mm when working for 10 s without GNSS signal.

5. 3D REFERENCE MODEL - TLS SURVEY

In order to provide a 3D reference dataset for the assessment of the systems presented in the last two sections, the interior of the Impossible bastion was fully surveyed with a Leica ScanStation C10 terrestrial laser scanner (TLS). Based on TOF measuring principle, this scanning system combines all-in-one portability with the ability of performing total station-like surveys (traverse and resection). The laser features full $360^\circ \times 270^\circ$ field-of-view thanks to the adoption of Smart X-Mirror design, low beam divergence (<6 mm @ 50 m), high accuracy (6 mm @ 50 m), long range (300 m @90% reflectivity), dual-axis compensator and high scan speed (50k pts/sec). In addition, the total station-like interface and on-board graphic colour touch screen display allow users on-site data viewing. Moreover, this scanner also has internal memory storage of 80 Gigabytes which is ideal for large area surveying.

The laser survey of the fortification was carried out by using the traversing method. This surveying procedure allows the user to take advantage of the Leica C10 built-in dual-axis compensator to use conventional surveying techniques to perform a traverse, and establishing relationships between successive scanner positions within a known or assumed coordinate system. Because the dual-axis compensator automatically corrects scan data for the vertical, the traverse procedure does not require as many targets as regular target-based registration. An open traverse consisting of 9 laser stations was set up to completely cover the study area.

On each station the laser scanner was set on a tripod and then carefully leveled and plumbed directly over the top of the traverse mark on the ground. Levelling of the instrument is required in order to enable automatic registration of acquired scans and to minimize measurement errors. After setting out the TLS, bearing and coordinates of the back station were set in order to define the fore station. Position of back and fore stations were measured by the laser scanner using proper Leica target poles (Fig. 3(b)), whose sizes are automatically stored in the laser firmware.

In order to meet the requirement of a clear line of sight between each target station (back and fore) and the laser station, scanner positions were carefully designed by taking into account the inner geometry of the fortification. From each laser station a set of scans were acquired with an average spatial resolution of about 1cm at a distance of 10m. Following a few initial tests, this value was deemed the most suited to generate a 3D model with good level of detail for subsequent analyses.

The raw data collected with the ScanSation C10 were then imported in Leica Cyclone software for processing. First, the scan station sequence was assembled in the Cyclone Traverse Editor in order to build the traverse. To this aim, instrument and target heights were entered for each scanner position. After verification and validation, the traverse could be carried out. Following this step, a registration process was applied in order to transform all the individual scans into a single dataset using 6 parameters of a rigid-body transformation (Reshetyuk, 2009). However with traversing, some initial constraints between laser stations could be generated and used to strength the alignment among the scans, giving a very geometrically accurate 3D model. Indeed, at the end of traverse processing, the laser stations and associated point clouds were defined in a common reference frame. This way scans acquired from different locations resulted to be already spatially "close" to each other. In addition, the information about instrument levelling, stored at each scanner position within the scans, allowed to remove a degree of freedom in the computing of the spatial transformation parameters between laser stations. Thus, by exploiting both these kind of spatial information, scan alignment could be automatically performed. However, since the generation of a laser traverse is always affected by residual errors, the registration results achieved this way needed to be furtherly refined. To this aim, an iterative global alignment process, based on the well known ICP (Iterative Closest Point) algorithm, was applied to all the pre-registered scans (Besl and McKay, 1992, Chen and Medioni, 1992). After the refinement step, the average residual alignment error was reduced to few millimeters (Fig. 5), and a global point cloud of about 27 mil of points was obtained (Fig. 6). As such large amount of points was mainly due to the

high degree of overlap between adjacent scans, the global cloud was properly decimated in CloudCompare software, setting an average point spacing of 1 cm. A final point cloud of ca 3.8 mil of points was then generated.

Constraint ID	ScanWorld	ScanWorld	Type	Error Vector
Cloud/Mes...	100: Stazione ...	300: Stazione ...	Cloud: Cloud/Mesh - Cloud...	aligned [0.003 m]
Cloud/Mes...	200: Stazione ...	400: Stazione ...	Cloud: Cloud/Mesh - Cloud...	aligned [0.003 m]
Cloud/Mes...	200: Stazione ...	100: Stazione ...	Cloud: Cloud/Mesh - Cloud...	aligned [0.003 m]
Cloud/Mes...	200: Stazione ...	300: Stazione ...	Cloud: Cloud/Mesh - Cloud...	aligned [0.003 m]
Cloud/Mes...	400: Stazione ...	500: Stazione ...	Cloud: Cloud/Mesh - Cloud...	aligned [0.003 m]
Cloud/Mes...	400: Stazione ...	300: Stazione ...	Cloud: Cloud/Mesh - Cloud...	aligned [0.003 m]
Cloud/Mes...	500: Stazione ...	600: Stazione ...	Cloud: Cloud/Mesh - Cloud...	aligned [0.004 m]
Cloud/Mes...	600: Stazione ...	700: Stazione ...	Cloud: Cloud/Mesh - Cloud...	aligned [0.008 m]
Cloud/Mes...	300: Stazione ...	800: Stazione ...	Cloud: Cloud/Mesh - Cloud...	aligned [0.006 m]
Cloud/Mes...	800: Stazione ...	900: Stazione ...	Cloud: Cloud/Mesh - Cloud...	aligned [0.007 m]

Figure 6. Results of the registration refinement.

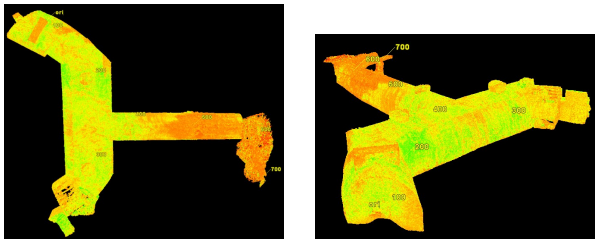

(a) (b)

Figure 7. Top view (a) and perspective view (b) of the decimated 3D model of Impossible bastion derived from TLS measurements. Intensity data are mapped onto the model with false color scale. Numbers denote traverse stations.

6. RESULTS AND DISCUSSION

Agisoft PhotoScan provided a reconstruction of 221 million points. Scaling factor has been estimated by comparing camera positions in the photogrammetric reconstruction and in the UWB positioning. Resulting estimated scale factor is 2.35, approximately.

Registration between TLS and photogrammetric reconstruction has been done with ICP algorithm. Resulting (RMSE) fitting error is 21.9cm, average error 13.4cm, and standard deviation 13.5cm. Fig. 8 shows how errors values are distributed over the bastion.

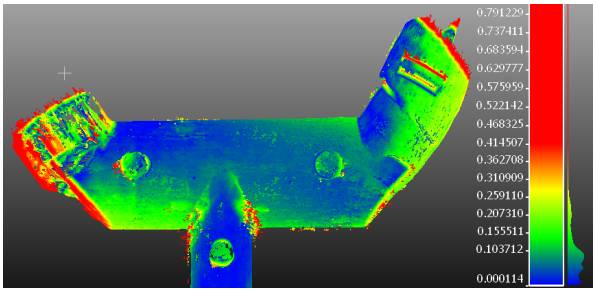

Figure 8. Error map for scale = 2.35. Figure was obtained from CloudCompare. Red values corresponds to higher error values. Values are saturated at 41cm (red values start approximately at 33cm, as shown in the color bar on the right).

As shown in Fig. 8, most critical areas are those at the final parts of the two bastion wings (left and right). Main reason for this is the error in the estimated scale factor between PhotoScan and metric reconstruction. This is confirmed by Fig. 9, which shows the error map when considering scale factor = 2.27: this scale factor value has been experimentally derived in order to obtain best fit between PhotoScan and TLS reconstruction. It is quite apparent that scaling factor used in Fig. 8 allows to obtain a better fitting than in Fig. 8. RMSE fitting error in this case is 12.3cm, average error 3.6cm, and standard deviation 7.8cm.

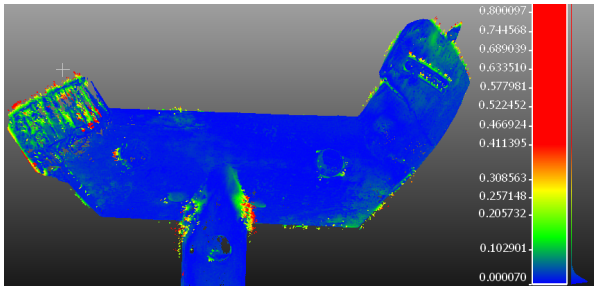

Figure 9. Error map for scale = 2.27. Figure was obtained from CloudCompare. Red values corresponds to higher error values. Values are saturated at 41cm (red values start approximately at 33cm, as shown in the color bar on the right).

It is worth to notice that some error peaks are still present in Fig. 9, mostly due to reconstruction noise. Actually, a critical part in this reconstruction is given by the final part of bastion left wing, shown in Fig. 9: this area is intrinsically quite complex to reconstruct, as visible in Fig. 10.

Figure 10. Final part of bastion left wing.

Excluding the area shown in Fig. 10 from validation, the resulting (RMSE) fitting error is 17.3cm, average error is 11.5cm, and standard deviation is 9.5cm for scale factor = 2.35. Instead, the following results are for scale factor = 2.27: RMSE = 8.4cm, average error = 2.4cm, and standard deviation = 3.1cm.

Instead, comparison between Leica backpack ans TLS surveys leads to the following results: average error = 4.7cm, and standard deviation = 0.6cm. As shown in Fig. 11, the most critical area is that on the left wing, again. Excluding such area from the analysis leads to: average error = 4.2cm, and standard deviation = 0.3cm.

7. CONCLUSIONS

This paper compared indoor surveys of a medieval bastion in Padua done by means of (i) TLS, (ii) photogrammetric, and (iii) Leica pegasus backpak reconstruction, where metric scale in the photogrammetric case is provided by a UWB based positioning system.

The rationale of the latter is basically that of developing a low cost system for indoor surveys, which requires only a minimal hu-

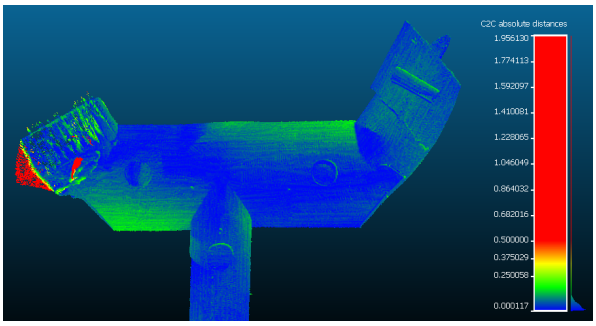

Figure 11. Error map backpack vs TLS survey. Figure was obtained by using CloudCompare. Red values corresponds to higher error values. Values are saturated at 50cm (red values start approximately at 38cm, as shown in the color bar on the right).

man expertise and effort in its use. Metric scale in this case is obtained by comparing camera positions in the structure from motion reconstruction (obtained by Agisoft PhotoScan) with those obtained by the considered UWB system. Pozyx UWB devices provided range measurements, which were processed off-line. Pozyx rover was attached to the camera during image acquisitions. Camera altitude was approximately constant during the survey, hence its altitude was set to a known constant value in the positioning algorithm in order to obtain best 2D positioning performance. Scale factor estimated with this method, i.e. 2.35, is only quite close to the best fitting one (e.g. 2.27). Improving positioning method, for instance introducing different weights for the UWB estimates, should allow to obtain better estimates of the scale factor and will be object of our future investigation.

Error on the scale causes a RMSE on the overall photogrammetric reconstruction of 21.9cm, whereas the use of scale factor = 2.27 leads to 12.3cm RMSE. Area shown in Fig. 10 is that causing most of the largest errors. Excluding that from the validation RMSE reduces to 17.3cm with scale factor = 2.35 (and 8.4cm with scale factor = 2.27). Applying some more smoothing to the photogrammetric reconstruction might probably allow to reduce the presence of certain isolated large errors due to large values of reconstruction noise.

Comparison of Leica backpack survey with the TLS 3D model leads to an average error of 4.7cm and standard deviation 0.6cm. Similarly to the photogrammetric case, error is slightly reduced by excluding the final part of the left wing: average error = 4.2cm and standard deviation = 0.3cm. It is worth to notice that these errors are actually quite compatible with our expectetions of such system given its tehcnical specifications in absence of GNSS signal: indeed, its positioning system error is nominally 20 mm after 10 s without GNSS signal. Given unavailability of the GNSS signal inside of the bastion the error between the Leica backpack and the TLS surveys might probably be mostly due to the positioning system error.

8. ACKNOWLEDGMENTS

The authors acknowledge the key account manager of Leica Geosystems (Hexagon) Giovanni Abate for his precious help in supporting us during the development of this project.

REFERENCES

Al Hamad, A. and El Sheimy, N., 2014. Smartphone based mobile mapping systems. ISPRS - International Archives of the Photogrammetry, Remote Sensing and Spatial Information Sciences XL-5, pp. 29–34.

Ballarin, M., Balletti, C., Faccio, P., Guerra, F., Saetta, A. and Vernier, P., 2017. Survey methods for seismic vulnerability assessment of historical masonry buildings. ISPRS - International Archives of the Photogrammetry, Remote Sensing and Spatial Information Sciences XLII-5/W1, pp. 55–59.

Besl, P. and McKay, N., 1992. A method for registration of 3-D shapes. IEEE Transactions on Pattern Analisys and Machine Intelligence 4(2), pp. 239–256.

Chen, Y. and Medioni, G., 1992. Object modelling by registration of multiple range images. Image and Vision Computing 10(3), pp. 145–155.

Chiang, K.-W., Tsai, M.-L. and Chu, C.-H., 2012. The development of an UAV borne direct georeferenced photogrammetric platform for ground control point free applications. Sensors 12(7), pp. 9161–9180.

Dierenbach, K., Ostrowski, S., Jozkow, G., Toth, C., , Grejner-Brzezinska, D. and Koppanyi, Z., 2015. UWB for navigation in GNSS compromised environments. In: Proceedings of the 28th International Technical Meeting of The Satellite Division of the Institute of Navigation (ION GNSS+ 2015), pp. pp. 2380–2389.

El-Sheimy, N. and Schwarz, K., 1998. Navigating urban areas by VISAT–A mobile mapping system integrating GPS/INS/digital cameras for GIS applications. Navigation 45(4), pp. 275–285.

Fissore, F., Pirotti, F. and Vettore, A., 2017. Open source web tool for tracking in a low cost MMS. ISPRS - International Archives of the Photogrammetry, Remote Sensing and Spatial Information Sciences.

Fraser, C. and Stamatopoulos, C., 2014. Automated target-free camera calibration. In: Proceedings of the ASPRS 2014 Annual Conference (Louisville, KY, USA), Vol. 2328.

Goel, S., Kealy, A., Gikas, V., Retscher, G., Toth, C., Brzezinska, D.-G. and Lohani, B., 2017. Cooperative localization of unmanned aerial vehicles using GNSS, MEMS inertial, and UWB sensors. Journal of Surveying Engineering 143(4), pp. 04017007.

Guarnieri, A., Masiero, A., Vettore, A. and Pirotti, F., 2015. Evaluation of the dynamic processes of a landslide with laser scanners and bayesian methods. Geomatics, Natural Hazards and Risk 6(5-7), pp. 614–634.

Habib, A. and Morgan, M., 2003. Automatic calibration of low-cost digital cameras. Optical Engineering 42(4), pp. 948–955.

Heikkila, J. and Silven, O., 1997. A four-step camera calibration procedure with implicit image correction. In: Computer Vision and Pattern Recognition, 1997. Proceedings., 1997 IEEE Computer Society Conference on, pp. 1106–1112.

Hol, J., 2011. Sensor Fusion and Calibration of Inertial Sensors, Vision, Ultra-Wideband and GPS. PhD. Thesis, Linköping University, The Institute of Technology.

Luhmann, T., Fraser, C. and Maas, H.-G., 2015. Sensor modelling and camera calibration for close-range photogrammetry. ISPRS Journal of Photogrammetry and Remote Sensing 115, pp. 37–46.

Masiero, A., Fissore, F. and Vettore, A., 2017. A low cost UWB based solution for direct georeferencing UAV photogrammetry. Remote Sensing 9(5), pp. 414.

Masiero, A., Fissore, F., Pirotti, F., Guarnieri, A. and Vettore, A., 2016. Toward the use of smartphones for mobile mapping. Geo-Spatial Information Science 19(3), pp. 210–221.

Masiero, A., Guarnieri, A., Pirotti, F. and Vettore, A., 2015. Semi-automated detection of surface degradation on bridges based on a level set method. ISPRS - International Archives of Photogrammetry, Remote Sensing and Spatial Information Sciences 40(3), pp. 15–21.

Piras, M., Di Pietra, V. and Visintini, D., 2017. 3D modeling of industrial heritage building using COTSs system: Test, limits and performances. Vol. 42, pp. 281–288.

Pirotti, F., Guarnieri, A. and Vettore, A., 2013. State of the art of ground and aerial laser scanning technologies for high-resolution topography of the earth surface. European Journal of Remote Sensing 46, pp. 66–78.

Remondino, F. and Fraser, C., 2006. Digital camera calibration methods: considerations and comparisons. ISPRS - International Archives of the Photogrammetry, Remote Sensing and Spatial Information Sciences XXXVI-5, pp. 266–272.

Remondino, F., Barazzetti, L., Nex, F., Scaioni, M. and Sarazzi, D., 2011. UAV photogrammetry for mapping and 3D modeling–current status and future perspectives. ISPRS - International Archives of the Photogrammetry, Remote Sensing and Spatial Information Sciences 38(1), pp. C22.

Remondino, F., Guarnieri, A. and Vettore, A., 2005. 3D modeling of close-range objects: photogrammetry or laser scanning? In: Electronic Imaging 2005, International Society for Optics and Photonics, pp. 216–225.

Reshetyuk, Y., 2009. Self-Calibration and Direct Georeferencing in Terrestrial Laser Scanning. Stockholm Royal Institute of Technology.

Saeedi, S., Moussa, A. and El-Sheimy, N., 2014. Context-aware personal navigation using embedded sensor fusion in smartphones. Sensors 14(4), pp. 5742–5767.

Toth, C., 2001. Sensor integration in airborne mapping. In: Instrumentation and Measurement Technology Conference, 2001. IMTC 2001. Proceedings of the 18th IEEE, Vol. 3, IEEE, pp. 2000–2005.

Toth, C., Jozkow, G., Ostrowski, S. and Grejner-Brzezinska, D., 2015. Positioning slow moving platforms by UWB technology in GPS–challenged areas. In: The 9th International Symposium on Mobile Mapping Technology, MMT 2015.

Widyawan, Pirkl, G., Munaretto, D., Fischer, C., An, C., Lukowicz, P., Klepal, M., Timm-Giel, A., Widmer, J., Pesch, D. and Gellersen, H., 2012. Virtual lifeline: Multimodal sensor data fusion for robust navigation in unknown environments. Pervasive and Mobile Computing 8(3), pp. 388–401.